Journal of Cleaner Production 277 (2020) 123275

Contents lists available at ScienceDirect

Journal of Cleaner Production

journal homepage: www.elsevier.com/locate/jclepro

Global socioeconomic exposure of heat extremes under climate change

Jie Chen [a, b], Yujie Liu [a, b, *], Tao Pan [a], Philippe Ciais [c], Ting Ma [d], Yanhua Liu [a], Dai Yamazaki [e], Quansheng Ge [a, b], Josep Peñuelas [f, g]

[a] Key Laboratory of Land Surface Pattern and Simulation, Institute of Geographic Sciences and Natural Resources Research, Chinese Academy of Sciences (CAS), Beijing, China
[b] University of Chinese Academy of Sciences (UCAS), Beijing, China
[c] Laboratoire des Sciences Du Climat et de L'Environnement, IPSL-LSCE CEA CNRS UVSQ, Gif-sur-Yvette, France
[d] State Key Laboratory of Resources and Environmental Information System, Institute of Geographic Sciences and Natural Resources Research, Chinese Academy of Sciences (CAS), Beijing, China
[e] Institute of Industrial Sciences, University of Tokyo, Tokyo, Japan
[f] CSIC, Global Ecology CREAF-CSIC-UAB, Bellaterra, 08193, Barcelona, Catalonia, Spain
[g] CREAF, Cerdanyola Del Vallès, 08193, Barcelona, Catalonia, Spain

ARTICLE INFO

Article history:
Received 10 November 2019
Received in revised form
7 June 2020
Accepted 10 July 2020
Available online 31 July 2020

Handling editor: Bin Chen

Keywords:
Socioeconomic exposure
Heat extremes
Climate change
Population exposure
Gross domestic product (GDP) exposure

ABSTRACT

Growing evidence indicates that the risk of heat extremes will increase as climate change progresses and create a significant threat to public health and the economy. Socioeconomic exposure is the key component for assessing the risk of such events. To quantify socioeconomic exposure to heat extremes for 2016–2035 and 2046–2065, we use the projections of five global climate models forced by using three representative concentration pathways (RCPs) and projections of population and gross domestic product (GDP), and we take into account the geographic change in the distribution in shared socioeconomic pathways (SSPs). The exposure of the global population for 2046–2065 is the greatest under the RCP8.5-SSP3 scenario, up to $1037(\pm164) \times 10^9$ person-days, and the global GDP exposure for 2046–2065 is greatest under the RCP2.6-SSP1 scenario, up to $18(\pm2) \times 10^{15}$ dollar-days. Asia has the highest exposure among all continents for both population and GDP, accounting for over half of the global exposure. Africa has the largest increase in exposure, with the annual population and GDP exposures increasing by over 9- and 29-fold, respectively, compared with the base period (1986–2005). The effect of climate makes the dominant contribution (47%–53%) globally for the change in population exposure. Changes in the geographic distribution of GDP cause nearly 50% of the total change in GDP exposure for 2016–2035. Mitigating emissions of greenhouse gases, either at the level of the RCP2.6 scenario or at a more ambitious target, is essential for reducing socioeconomic exposure to heat extremes. In addition, designing and implementing effective measures of adaptation are urgently needed in Asia and Africa to aid socioeconomic systems suffering from heat extremes due to climate change.

1. Introduction

Climatic extremes cause extensive economic damage each year, and the risks are expected to increase with continued socioeconomic development and climate change. Risk is usually represented as the probability of occurrence of hazardous events or trends multiplied by the impact if these events or trends occur. Risk is due to the interaction of hazard, exposure, and vulnerability. Exposure usually refers to the people, livelihoods, resources, infrastructure, and economic, social, or cultural assets in places and settings that could be adversely affected (IPCC, 2014). The prediction of changes in exposure to future climatic extremes could, therefore, contribute to the need to consider effective countermeasures to reduce vulnerability and risk. Global socioeconomic exposure (i.e., exposure of the population and gross domestic product, GDP) under climate change has received less attention (Burke et al., 2015; Carleton and Hsiang, 2016), despite recent progress in assessing the hazards of climatic extremes (Hirabayashi

* Corresponding author. No.11A, Datun Road, Chaoyang District, Beijing, China.
E-mail address: liuyujie@igsnrr.ac.cn (Y. Liu).

https://doi.org/10.1016/j.jclepro.2020.123275
0959-6526/

et al., 2013; Cook et al., 2014; King et al., 2017; Huang et al., 2017; Nath et al., 2017). Such estimates are urgently needed to clarify future spatiotemporal variation and changes in global socioeconomic exposure and thereby avoid adverse effects on public health and the economy. The importance of assessing exposure is gradually being recognized, as indicated by the published reports of the Intergovernmental Panel on Climate Change (Field et al., 2012; IPCC, 2013), the proposal of a new set of shared socioeconomic pathways (SSPs, O'Neill et al., 2014), and some recent studies of the risk of climate change that considers the effects of socioeconomic factors (Ceola et al., 2015; Mora et al., 2017; Zhang et al., 2018a). The integration of climate change with the social economy to estimate future risk, the assessment of the relative importance of different factors, and the quantification of uncertainty would provide a basis for adapting to extreme climate change and reducing the risk of heat extremes.

Because of climate change, the frequency and intensity of climatic extremes, such as heat extremes, have increased in recent decades and are likely to continue to increase in the coming decades (IPCC, 2013). Heat extremes have been responsible for significant public health threats and economic losses over the last 100 years. Data for historical damage from the International Disaster Database (https://www.emdat.be/emdat_db/) indicate that heat extremes affected 1.03×10^8 people, which includes the deaths of 183 495 people, and caused worldwide economic losses of 6.33×10^{10} USD from 1936 to 2019. Serious heat extremes have also occurred more frequently in recent decades, such as those in Europe in 2003, 2018 and 2019 (Robine et al., 2008), Australia in 2008 (Vaneckova et al., 2008), Russia in 2010 (Trenberth and Fasullo, 2012), and China in 2013 (Sun et al., 2014). Socioeconomic exposure and disaster risks will be magnified in a warmer future (Jones, and O'Neill, 2016; Smirnov et al., 2016), when the more frequent and intense heat extremes of this century (Fischer and Knutti, 2015; Kharin et al., 2013) combine with a greater population and the accumulation of wealth.

In socioeconomic systems, population is most closely related to heat extremes because of its direct impact on public health (Wang et al., 2019). Various economic sectors also can be seriously affected by heat extremes, such as agriculture (water shortages) and industries that rely heavily on hydropower. In addition, tourism, transportation, construction, and other industries are also affected by heat extremes to varying degrees (IPCC, 2014). Considering the data on historical damage of heat extremes (number of people affected, total damage on the economy, etc.) and the availability of simulated socioeconomic data for the future, we selected population and economic activity, expressed as GDP, to determine the impact of heat extremes on the socioeconomic system. Many studies that have quantified future socioeconomic exposure have not considered changes in populations or GDP but assumed that these variables remain constant, which is inappropriate for predicting changes in exposure (Bouwer, 2013; Sun et al., 2017). Most studies have also focused on changes in exposure based on a specific pathway of emission of a greenhouse gas (GHG) or a target of global mean temperature (GMT) rise such as 1.5 °C or 2.0 °C (Harrington and Otto, 2018; Mishra et al., 2017). These analyses of the spatiotemporal variation in exposure between scenarios and time periods are thus insufficient because the population and economy (usually calculated by GDP) are both essential elements in socioeconomic systems and are the factors most severely affected by climatic extremes. The exposures of populations and GDP are usually predicted separately, and these two elements are rarely used to assess socioeconomic exposure (Bowles et al., 2014; Forzieri et al., 2017), although the spatial distributions of populations and economies are also consistent. Given these factors, we focus in this work on simulating the global exposure to extreme heat as a function of changes in climate and population or GDP. The results constitute a first step toward understanding how interactions between climate change and socioeconomic systems affect exposure patterns.

This study systematically quantify the global spatiotemporal distribution of and changes in exposure of population and GDP to heat extremes under different scenarios and over different time periods. Bias-corrected projections of five global climate models (GCMs, Table 1) driven by representative concentration pathways (RCPs) are used to calculate the frequency of extreme heat events (see Sec. 2.1, Materials). Combined with population and GDP projections in SSPs (Figs. S1 and S2), which consider changes in the geographic distribution of population and GDP (see Sec. 2.1, Materials), the spatiotemporal variation of global exposure to extreme heat of the population and GDP is quantified in both the base period (1986–2005) and in future periods (2016–2035 and 2046–2065) under various scenarios (see Sec. 2, Materials and Methods). We also assess the relative importance of climatic and socioeconomic factors and their uncertainties to characterize the contribution of climate change and growth in population and GDP to future changes in extreme-heat exposure. The main target of this study is quantifying the impact of heat extremes on socioeconomic system under climate change to characterize variation of socioeconomic exposure among scenarios and periods, distinguish high exposure regions, and identify dominant contributor for exposure change, so as to support policymakers in the development of climate change mitigation and adaptation strategies.

2. Materials and Methods

2.1. Materials

Daily climatic data were obtained from the Inter-Sectoral Impact Model Intercomparison Project (ISI-MIP, Warszawski et al., 2014) for the Coupled Model Intercomparison Project Phase 5 (CMIP5, Taylor et al., 2012) (Table 1), which contains simulations from five GCMs based on RCPs. The RCP scenarios represent pathways based on simulated impacts on land use, aerosol emissions, and GHGs (Vuuren et al., 2011). The four RCPs cover the period up to 2100 and have radiative forcings from the open literature that vary from 2.6 to 8.5 W/m^2. The scenarios, RCP2.6, RCP4.5, and RCP8.5, which represent low, middle, and high GHG emissions, respectively, were selected for analysis (Vuuren et al., 2011). RCP6.0, which is interpreted as either a medium baseline or a high-mitigation case between RCP4.5 and RCP8.5, is not used. The base period was 1986–2005, which is the commonly used reference period in assessments of projected changes in extreme indices and climate impacts (Schleussner et al., 2016). Future periods in the 2030s and 2050s were given lengths of 20 years (2016–2035 and 2045–2065) to be consistent with the base period. The spatial resolution of the output data was offset-corrected and converted to $0.5^\circ \times 0.5^\circ$ latitude and longitude by spatial downscaling. Statistical bias-correction methods facilitate the comparison between observed and simulated data during the historical reference period and for a continuous transition into the future (Hempel et al., 2013). Preservation of absolute changes in monthly temperature and relative changes in monthly precipitation in each grid cell implies that the global warming trend and the climate sensitivities of the GCMs are preserved, and the trend and the long-term mean are well represented, which ensures the credibility of the simulated data (Hempel et al., 2013; Warszawski et al., 2014).

The United Nations, the World Bank, and other organizations proposed future socioeconomic projections for population and GDP. Many previous studies also combined current socioeconomic data with future climatic data for analysis, although these studies

Table 1
Description of global climate models (GCMs).

Model	Institute	Atmospheric resolution (longitude × latitude)
GFDL-ESM2M	Geophysical Fluid Dynamics Laboratory	2.5° × 2°
HadGEM2-ES	National Institute of Meteorological Research/Korea Meteorological Administration	1.875° × 1.25°
IPSL-CM5A-LR	Institute Pierre-Simon Laplace	3.75° × 1.875°
MIROC-ESM-CHEM	Japan Agency for Marine-Earth Science and Technology, Atmosphere and Ocean Research Institute (University of Tokyo), and National Institute for Environmental Studies	2.8° × 2.8°
NorESM1-M	Norwegian Climate Centre	2.5° × 1.89°

neglected to consider how changes in socioeconomic factors affect exposure. We used the predictions of population and GDP from the scenarios of SSPs based on the selected RCP scenarios. SSPs are reference pathways describing possible alternative trends in the evolution of societies and ecosystems on a timescale of 100 years without climate change or implementation of climate policies (Riahi et al., 2017). RCP2.6, 4.5, and 8.5 generally correspond to SSP1, 2, and 3, respectively, based on the correspondence between the RCPs and SSPs provided by the IPCC (O'Neill et al., 2014; Table S4). We therefore selected SSP1, 2, and 3 for this study. The RCP2.6-SSP1 scenario assumes low carbon emissions, sustainable development proceeding at a reasonably high pace, and fewer inequalities. The RCP4.5-SSP2 scenario assumes moderate carbon emissions with medium growth in population and GDP. Finally, the RCP8.5-SSP3 scenario assumes high carbon emissions with a rapidly growing population and a low adaptive capacity. The projections of population and GDP were obtained from the National Institute for Environmental Studies, Japan (NIES), which were downscaled from the International Institute for Applied Systems Analysis (IIASA). The spatial resolution was also 0.5° × 0.5° latitude and longitude. The population and GDP projections were downscaled with explicitly considered spatial and socioeconomic interactions between cities, and they used auxiliary variables, including road network and land cover. The downscaling results were consistent with the scenario assumptions and captured the difference in urban and non-urban areas in a more reasonable manner, which ensures the prediction accuracy of the SSPs (Murakami and Yamagata, 2016).

2.2. Methods

2.2.1. Hazards of extreme heat

Annual days of extreme heat, which is also the frequency of extreme heat, were used to quantify the hazard, which is defined as the daily maximum temperature exceeding a threshold. The threshold for extreme heat was defined as the 90th percentile of daily maximum temperatures for the base period (1986–2005) and was set at 25 °C when the local 90th percentile was <25 °C (Garssen et al., 2005). We chose relative thresholds rather than a fixed threshold to project global spatiotemporal variation and changes in exposure because no single fixed threshold suffices for the substantial differences in climatic conditions around the world (Gasparrini et al., 2015). Relative thresholds were, therefore, the simplest definitions of regionally relevant extreme heat around the globe. The frequency of extreme heat was calculated as follows:

$$C = \sum_{i=1}^{365} (TEM_i > THR), \quad (1)$$

$$\overline{C} = \frac{\sum_{j=1}^{5} C_j}{5}, \quad (2)$$

where C is the annual number of days of extreme heat (day), i is the ith day of a year, TEM is the daily maximum temperature (°C), THR is the local threshold (°C), $\overline{C}$ is the multi-model averaged value of C(day), and j is the jth GCM.

2.2.2. Exposure to extreme heat

We measured population and GDP exposure for each grid cell as the number of extreme heat days multiplied by the number of people and GDP, respectively (Jones et al., 2015). Therefore, the units of population and GDP exposures are person-days and purchasing power parity (PPP) dollar-days, respectively. To calculate exposure in the base period and in the future periods (2016–2035 and 2046–2065), we minimized interannual variations by using 20-year averages of annual extreme heat days and of the projections of population and GDP. The 20-year mean exposure for each projection of the five climate models was calculated for the base period and for the future periods. Moreover, exposure for the grid cells was also aggregated to global and continental scales for further analysis. Explicitly, we have

$$\overline{E_P} = \frac{\sum_{m=1}^{20} C_m \times P}{20}, \quad (3)$$

$$\overline{E_G} = \frac{\sum_{m=1}^{20} C_m \times G}{20}, \quad (4)$$

where $\overline{E_P}$ is the 20-year-averaged population exposure (person-day), m is the mth year of the study period, C is the number of annual days of extreme heat (day), P is the simulated population number (person), $\overline{E_G}$ is the 20-year-averaged GDP exposure (PPP $-day), and G is the GDP simulation (PPP $).

2.2.3. Analysis of relative importance of change in exposure and cumulative probability

Using techniques from a previous study (Jones et al., 2015), we evaluated the relative importance of the effects of different factors by categorizing the changes in population and GDP exposures in terms of the effects of climate, population, GDP, and interactions. The impact of population and GDP was calculated by holding climate constant (i.e., the 20 year averages of annual days of extreme heat for the base period were multiplied by the populations and GDPs in the RCP-SSP scenarios). Population and GDP were similarly held constant when calculating the impact of climate (i.e., the population for the base period was multiplied by the 20 year averages of annual days of extreme heat in the RCP

scenarios). The interactive effect was also calculated to determine whether the areas with continued population and GDP growth experienced more heat extremes under climate change. The changes in population and GDP exposure were categorized as follows:

$$\Delta E_P = C_b \Delta P + P_b \Delta C + \Delta P \Delta C, \quad (5)$$

$$\Delta E_G = C_b \Delta G + G_b \Delta C + \Delta G \Delta C, \quad (6)$$

where ΔE_P is the total change in population exposure, $\Delta E_G$is the total change in GDP exposure, $C_b$is the annual days of extreme heat for the base period, P_b and G_b are the population and GDP for the base period, respectively, $\Delta C$is the change in annual days of extreme heat from the base period to future periods, and ΔP and ΔG are the changes in population and GDP, respectively, from the base period to future periods. Therefore, $C_b \Delta P$ is the population effect, $C_b \Delta G$ is the GDP effect, $P_b \Delta C$ and $G_b \Delta C$ are the climatic effects, and $\Delta P \Delta C$ and $\Delta G \Delta C$ are the interactive effects.

The uncertainties of changes in population and GDP exposure for future scenarios were analyzed to evaluate the possible impact of climate change and growth on population and GDP. The probability analysis of changes in population and GDP were first separately calculated in each GCM based on the cumulative distribution function (CDF). Next, the mean value and standard deviation for the five GCMs were computed. The CDF of a random variable X represents the probability that $X \leq x$.

3. Results

3.1. Spatial pattern of population and GDP exposures to extreme heat

Fig. 1 shows the multi-model average exposures of the population and GDP for RCP8.5-SSP3 for 2046–2065. Fig. S3 shows the frequency of extreme heat, and Figs. S4 and S5 show the population and GDP exposures, respectively. Tables S1 and S2 present the statistics for population and GDP exposures globally and continentally for the RCP-SSP scenarios and the different time periods.

The spatial distribution of the frequency of heat extremes indicates latitudinal zonality in each time period and for each scenario (Fig. S3). The threshold in the base period exceeds 25 °C, except at latitudes >50° and on the Qinghai-Tibet Plateau. Heat extremes are most frequent near the equator, and their frequency gradually decreased with increasing latitude in both the base period and future periods. The frequency of extreme heat clearly increases over time. The highest frequency is 36.5 days in the base period, whereas the frequency is projected to exceed 120 days in the RCP scenarios. The frequency is significantly higher for 2046–2065 than 2016–2035 under each scenario. The frequency is highest under the RCP8.5 scenario and lowest under RCP2.6, but the difference between the scenarios is less than the difference between the time periods.

The regions with high population and GDP exposures to extreme heat are primarily concentrated in densely populated areas, such as India, China, midwestern Europe, the eastern USA, and the coastal areas of South America, for both the base period and the projected scenarios (Fig. 1). Exposure is also high near the equator in Africa because of the frequent occurrence of extreme heat. Population exposure under the RCP scenarios is highest for India and the east coast of China (>10 × 10^6 person-days). GDP exposure is much higher for eastern China, the Indian subcontinent, western Europe, and eastern North America than other locations such as northern Asia, northern North America, and Middle Oceania, with annual GDP exposure >100 × 10^9 PPP dollar-days.

3.2. Global and continental change in exposure to extreme heat

Annual exposure of the global population for the base period is 217.80 × 10^9 person-days, which increases to 1037.06 × 10^9 person-days for 2046–2065 under the RCP8.5-SSP3 scenario (Table S1). The increase in population exposure is largest for the RCP8.5-SSP3 scenario and smallest for RCP2.6-SSP1 (Fig. 2). The increase in global annual GDP exposure is largest for 2046–2065 under the RCP2.6-SSP1 scenario (Fig. 3), with a 10.47-fold increase in exposure relative to the base period (Table S2). In contrast, the increase is smallest for 2016–2035 under RCP8.5-SSP3, with an increase of only 3.71-fold relative to the base period. The reason that the highest GDP exposure appears in the RCP2.6-SSP1 scenario is that SSP1 is a "sustainable" scenario that assumes economic growth is shared at the global scale, so GDP increases relatively more in countries that currently have less wealth. Therefore, the exposed GDP at the global scale is higher in RCP2.6-SSP1, despite the hazard of extreme heat being lower in RCP2.6.

The population exposure is highest for Asia, followed by Africa, and lowest in Oceania in both the base period and the RCP scenarios. Exposure in Asia and Africa in the base period is 63% and 14%, respectively (Table S1). The percentage of population exposure

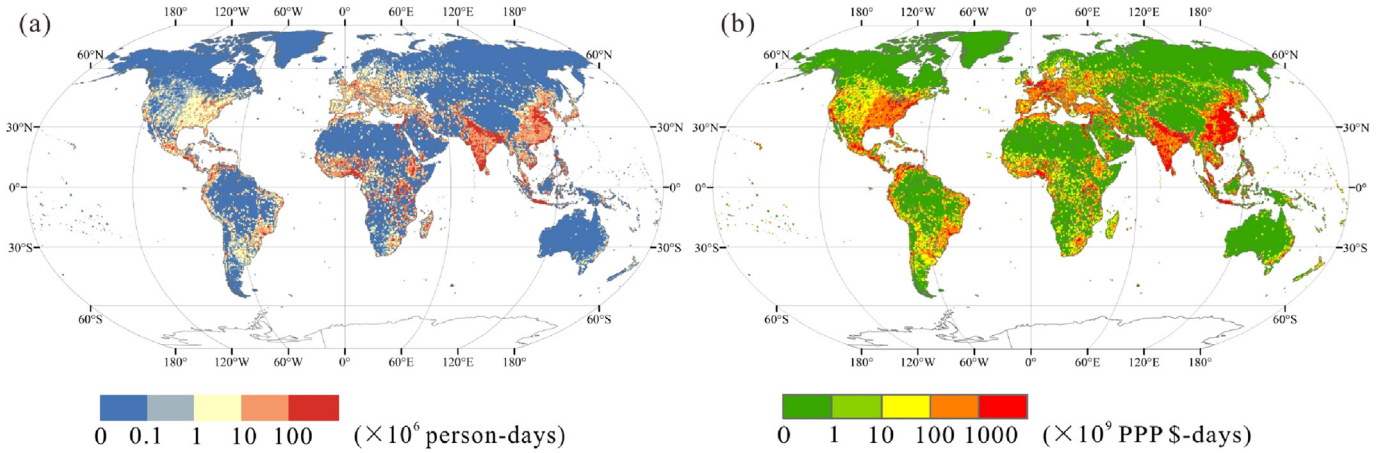

Fig. 1. Multi-model global projections of average exposures of (a) population and (b) GDP to extreme heat for the RCP8.5-SSP3 scenario for 2046–2065. PPP is purchasing power parity in USD.

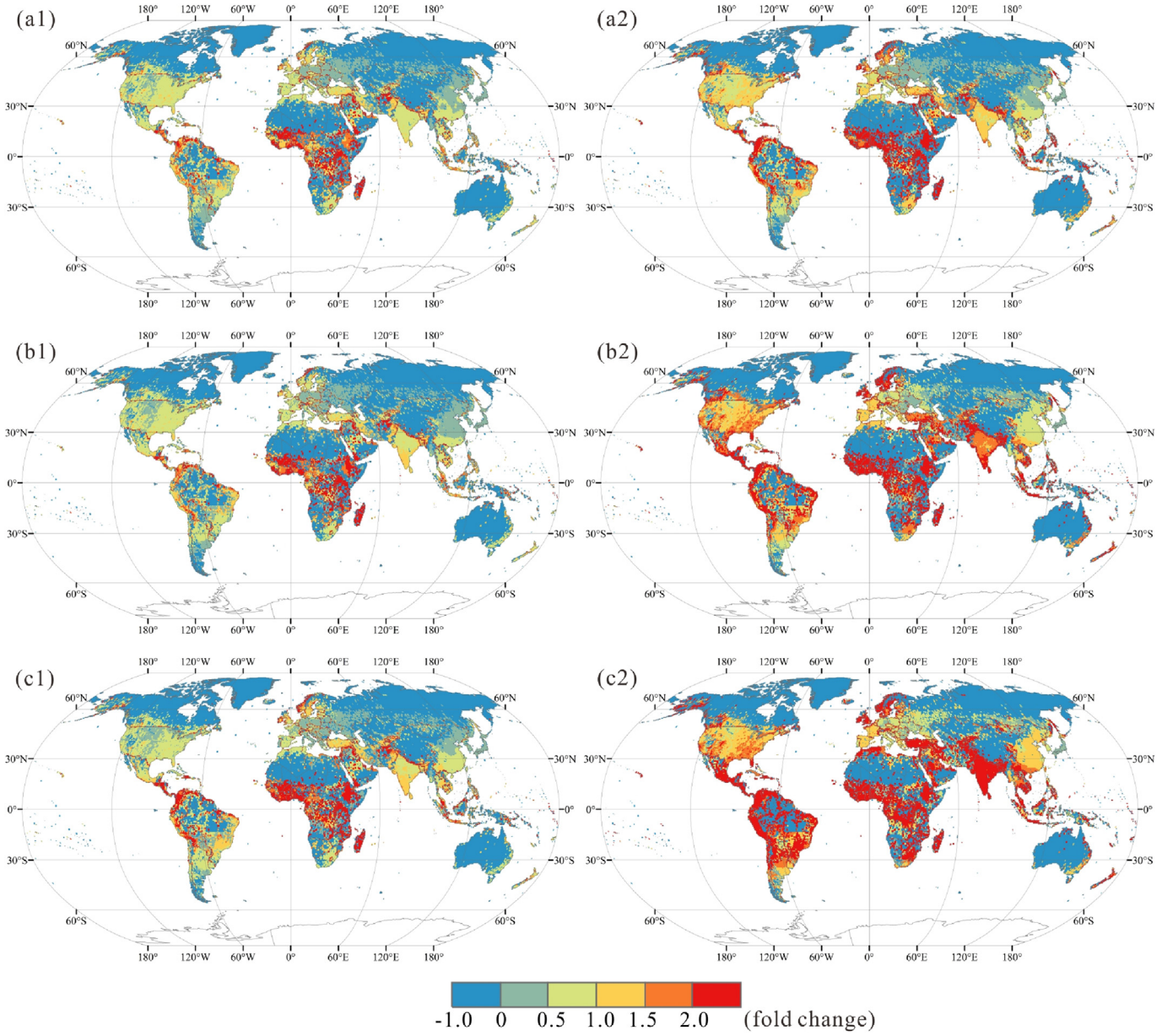

Fig. 2. Multi-model global projections of average relative change in population exposure to extreme heat for the three RCP scenarios and two time periods relative to the base period: (a) RCP2.6-SSP1, (b) RCP4.5-SSP2, (c) RCP8.5-SSP3, (1) 2016–2035, (2) 2046–2065.

under the three RCP scenarios decreases for Asia and increases for Africa. The percentage of population exposure for 2046–2065 under the RCP8.5-SSP3 scenario decreases for Asia to 53% and increases for Africa to 29% of global exposure. Exposure for the continental GDP in the base period ranks as follows: Asia > North America > Europe > South America > Africa > Oceania (Table S2).

The percent of GDP exposure increases for Asia, Africa, and South America and decreases for North America, Europe, and Oceania. The increase in both continental population and GDP exposures is largest for Africa, with the annual population exposure >9.20-fold higher under the RCP8.5-SSP3 scenario for 2046–2065 than for the base period, and the change of population exposure is 1.22-fold larger over the same period and under the same scenarios for Europe than in the base period, which is the smallest change among the continents. GDP exposure increases the most in Africa, by > 29.34-fold relative to the base period under the RCP2.6-SSP1 scenario for 2046–2065, whereas GDP exposure in North America is 3.99-fold higher for 2046–2065 than the base period, which is the lowest among continents.

Fig. 2 presents the relative changes in population exposure for the projected scenarios relative to the base period. The rate of change is highest in Africa in regions near the equator. Population exposure for 2016–2035 under the RCP2.6-SSP1 scenario increases more than 2-fold. The increase in the coastal regions of South America is also rapid, by more than 2-fold for 2046–2065 under the RCP4.5-SSP2 scenario. The rate of change, however, is <50% in areas where the rate has usually been high, such as China, the USA, and Western Europe. Population exposure is much higher for 2046–2065 than 2016–2035 under each scenario when the differences are compared between different time periods, with time, the population increases gradually, and when that increase is crossed with the more frequent heat extremes affected by climate change. Population exposure is highest under the RC8.5-SSP3 scenario, where population growth is rapid, followed by the RCP4.5-

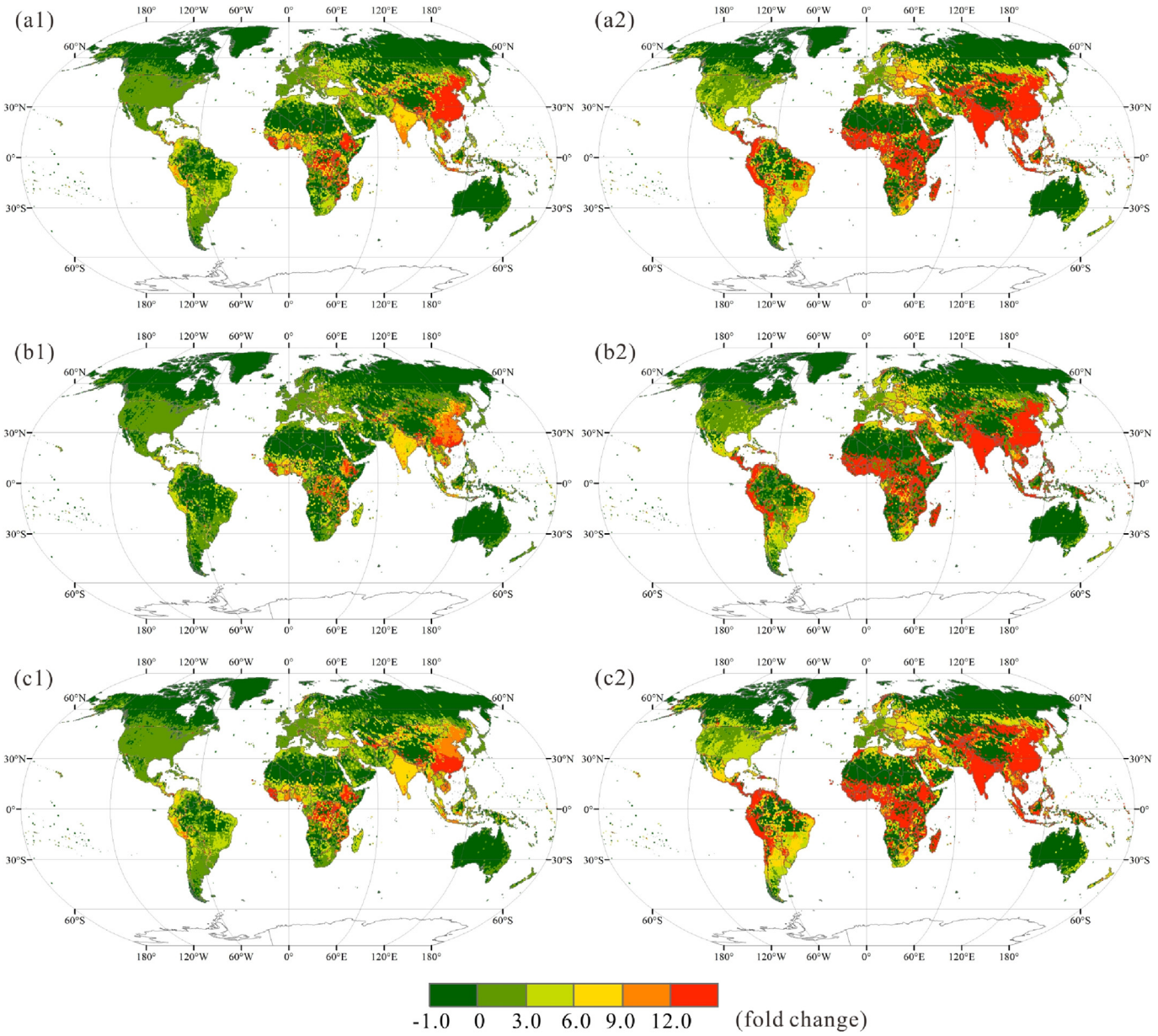

Fig. 3. Multi-model global projections of average relative change in GDP exposure to extreme heat for the three RCP scenarios and two time periods relative to the base period: (a) RCP2.6-SSP1, (b) RCP4.5-SSP2, (c) RCP8.5-SSP3, (1) 2016–2035, (2) 2046–2065.

SSP2 and RCP2.6-SSP1 scenarios.

Fig. 3 presents the spatial distributions of the average relative changes in GDP exposure for the RCP scenarios projected by multiple models. GDP exposure for 2016–2035 increases most rapidly in eastern China, with a more than 9-fold increase relative to the base period. GDP exposure also changes for central Africa and the South Asian subcontinent, with more than 6-fold increases relative to the base period. GDP exposure increases for 2046–2065 relative to the base period and 2016–2035. The increase in exposure is largest for Asia and is > 12-fold higher than the base period in many countries, such as China, India, and Mongolia. GDP exposure also changes for Africa, South America, and Eastern Europe. The change in exposure is relatively small for North America and Oceania, less than 6-fold relative to the base period. GDP exposure is highest under the RC2.6-SSP1 scenario, where GDP growth is fastest, followed by the RCP4.5-SSP2 and RCP8.5-SSP3 scenarios.

3.3. Analysis of relative importance of change in exposure

To determine the relative importance of various factors, we categorize the changes in population and GDP exposures in terms of the effects of population, GDP, climate, and their interactions. Figs. 4–6 show the changes in exposure and its components for the globe and for the continents under the three RCP scenarios. The change in global exposure of the population is primarily affected by the climate, whereas the change in global exposure of GDP is mainly attributed to the GDP effect (Fig. 4).

The climate effect accounts for nearly half of the total change in population exposure (47%–53%) in each scenario and for each period. The effect of population change for 2016–2035 is larger than the interactive effect, which reverses for 2046–2065. The GDP effect is responsible for nearly 50% of the total change in GDP exposure for 2016–2035, with approximately 30% and 20%

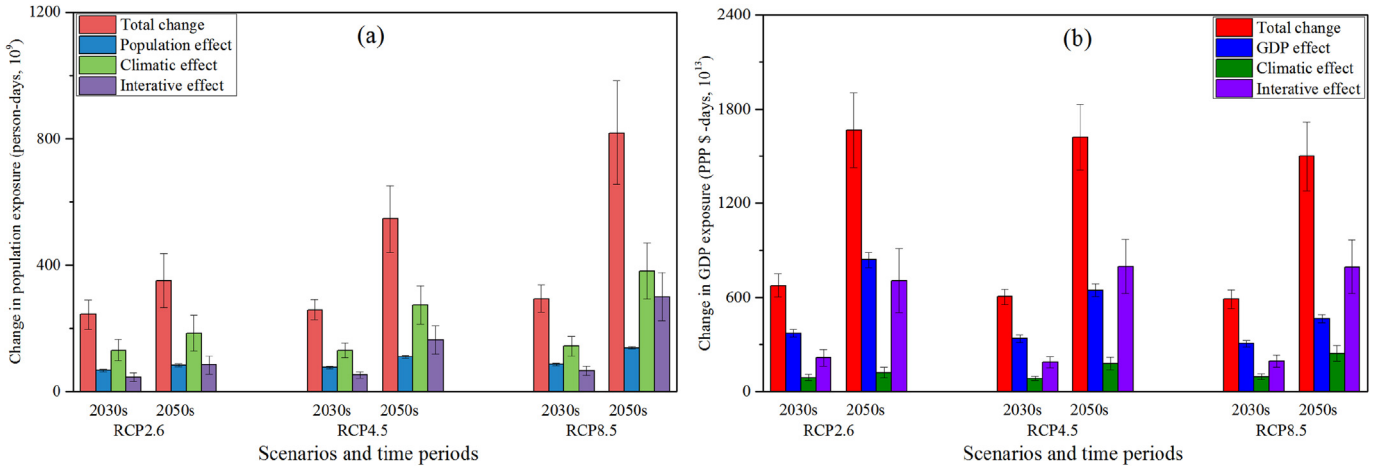

Fig. 4. Categorization of projected aggregate global changes in (a) population and (b) GDP exposure to extreme heat under the RCP2.6-SSP1, RCP4.5-SSP2, and RCP8.5-SSP3 scenarios. Error bars are the standard deviations for the results of the five GCMs. PPP is purchasing power parity in USD.

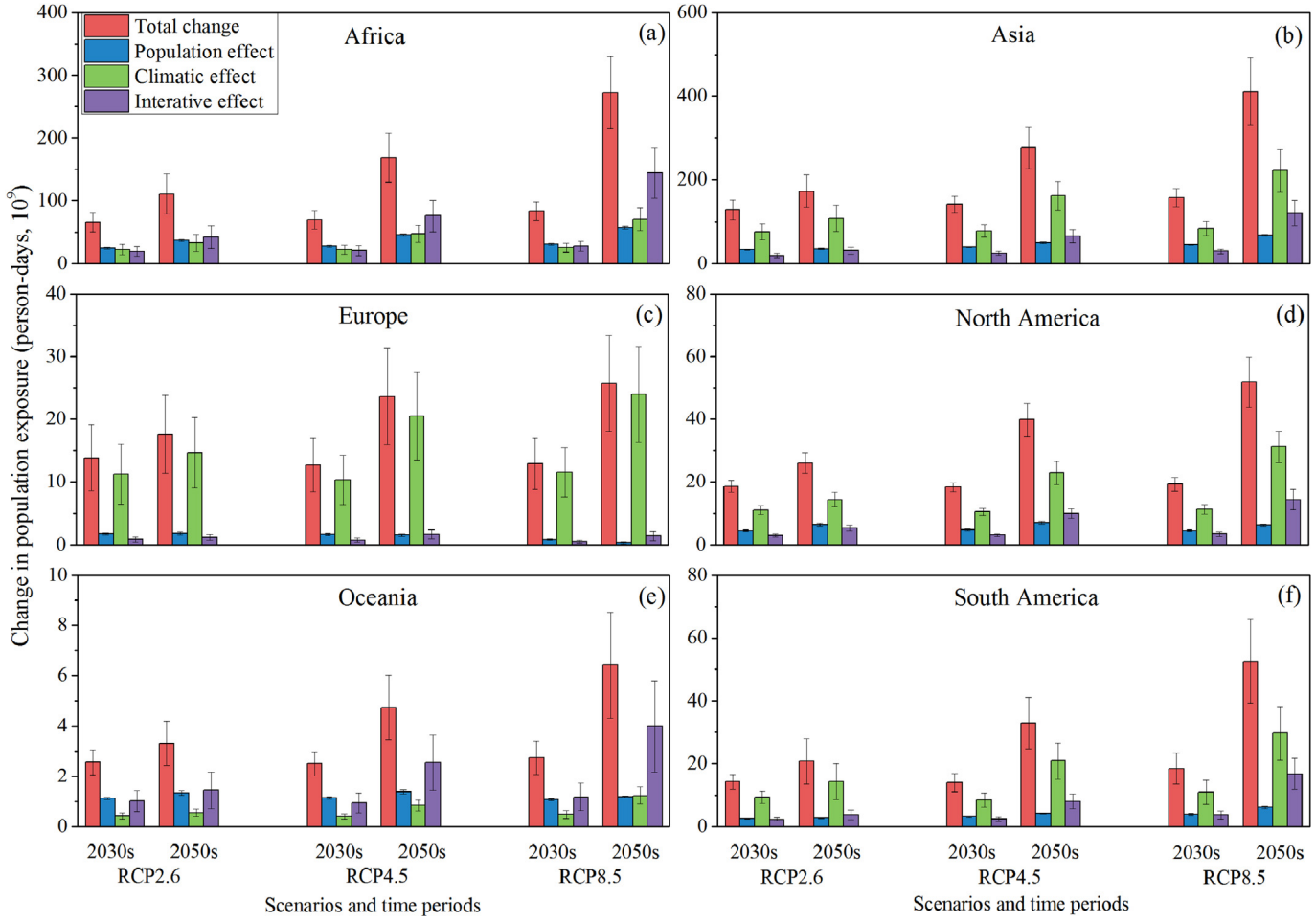

Fig. 5. Categorization of projected aggregate continental change in population exposure to extreme heat under the RCP2.6-SSP1, RCP4.5-SSP2, and RCP8.5-SSP3 scenarios. Error bars are the standard deviations for the results of the five GCMs: (a) Africa, (b) Asia, (c) Europe, (d) North America, (e) Oceania, (f) South America.

attributable to the effects of climate and interactions, respectively. The change in GDP exposure for 2046–2065 under the RCP4.5-SSP2 and RCP8.5-SSP3 scenarios is dominated by the interactive effect, at 49% and 53%, respectively, followed by the effects of GDP and climate. The increase in the influence of the interactive effect highlights the importance of the interactions between GDP and climate change in increasing GDP exposure under the scenarios of high GHG emissions.

The relative importance of the factors of change in population exposure at the continental level varies between regions (Fig. 5). As

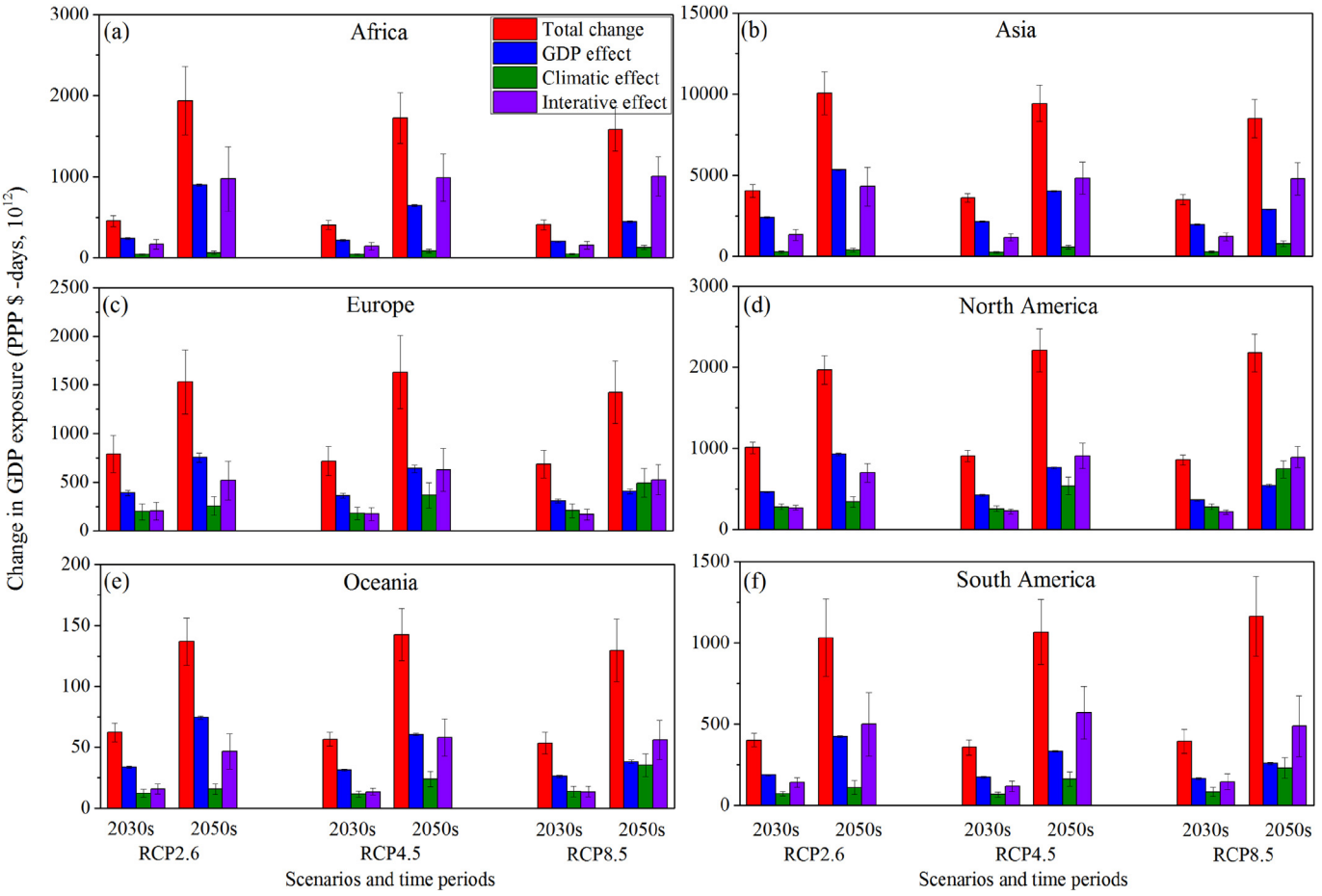

Fig. 6. Categorization of projected aggregate continental change in GDP exposure to extreme heat under the RCP2.6-SSP1, RCP4.5-SSP2, and RCP8.5-SSP3 scenarios. Error bars are the standard deviations for the results of the five GCMs. PPP is purchasing power parity in USD: (a) Africa, (b) Asia, (c) Europe, (d) North America, (e), Oceania, (f) South America.

noted above, the percent of population exposure worldwide is highest for Asia and Africa, but the dominant contribution to the change differs between the two continents. The effect of climate is the dominant contribution for Asia, Europe, North America, and South America for all scenarios and periods. This result indicates that an increased frequency of heat extremes amplifies population exposure, even in the absence of population increases on these continents. In contrast, the contribution of the three factors (i.e., the effects of population, climate, and the interaction) for Africa is nearly identical for 2016–2035 because of the strong population increase projected for this continent. The interactive effect, however, becomes the primary contribution for 2046–2065, particularly under the RCP8.5-SSP3 scenario, accounting for 53% of the total change, which is more than the sum of the population and interactive effects. The contributions of the GDP and interactive effects for Oceania are nearly the same for 2016–2035 under the three scenarios. In contrast, the interactive effect makes the primary contribution to the change in GDP exposure for 2046–2065 under the RCP4.5-SSP2 and RCP8.5-SSP3 scenarios.

Between continents, the differences in relative importance to GDP exposure to the effects of GDP, climate, and interactions are clear (Fig. 6), and the contribution of GDP, climatic, and interactive effects under the various scenarios and periods also varies among continents. The largest contribution for Asia and North America is from GDP for 2016–2035 under the three scenarios and for 2046–2065 under the RCP2.6-SSP1 scenario, whereas the interactive effect is the dominant contribution for 2046–2065 under the RCP4.5-SSP2 and RCP8.5-SSP3 scenarios. The GDP effect for Africa and South America is the primary contributor for 2016–2035, whereas the interactive effect is the primary contributor for 2046–2065. The difference between the interactive and GDP effects also increases for the pathways involving high GHG emissions in these two continents. The interactive effect for the RCP8.5-SSP3 scenario accounts for 64% of the total change for Africa, exceeding the contribution of 35% for the GDP effect. The interactive effect accounts for 58% of the total change for South America, whereas the GDP effect accounts for only 22%. The increase in GHG emissions leading to climate change and more frequent heat extremes can account for the increase in the difference between the interactive and GDP effects. The interaction between climate and change in GDP amplifies the exposure, but the GDP effect decreases, and the interactive effect increases as GDP growth slows under the pathways with high GHG emissions, which leads to the large difference between the effects under the RCP8.5-SSP3 scenario. The GDP effect is the primary contributor for Europe and Oceania for all periods and scenarios, except for 2046–2065 under the RCP8.5-SSP3 scenario, which implies that GDP exposure on these two continents would increase quickly without the impact of climate change. For almost all continents, GDP exposure is dominated by the GDP effect under the RCP2.6-SSP1 scenario because GDP grows fastest under this scenario.

3.4. Analysis of cumulative probability of changes in population and GDP exposures

Fig. 7 shows the cumulative distribution functions for changes in

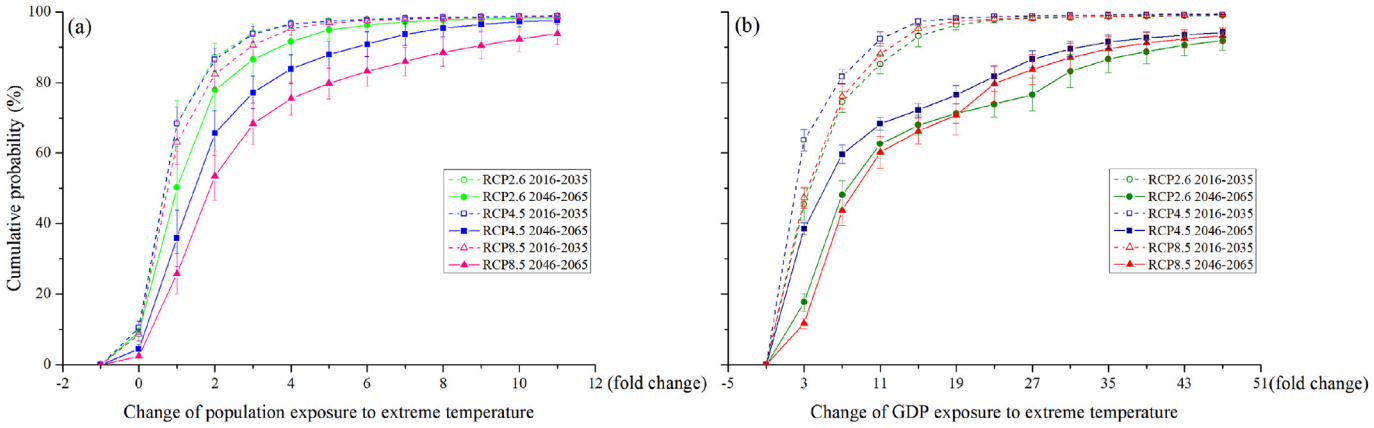

Fig. 7. Cumulative probability of projected change in (a) population exposure and (b) GDP exposure to extreme heat relative to the base period. Error bars are the standard deviations for the results of the five GCMs.

population and GDP exposures under the various scenarios and time periods relative to the base period. The changes are smaller for 2016–2035 than 2046–2065 for both population and GDP exposure, which indicates that population and GDP exposures increase rapidly over time, independent of the scenario. Population and GDP exposures, however, differ between the three scenarios and the two time periods. The cumulative probability of an increase in population exposure is >90% for 2016–2035 and > 95% for 2046–2065. The change is largest under RCP8.5-SSP3, with 90% probability of a zero-to 10-fold increase for both periods, followed by RCP4.5-SSP2 and RCP2.6-SSP1, with a 90% probability of a zero-to 7-fold increase relative to the base period. The future increase is much faster for GDP exposure than for population exposure because of the faster growth in GDP. The change in GDP exposure for 2046–2065 under the RCP2.6-SSP1 scenario is the largest among all time periods and scenarios, with 90% probability of a difference of −1- to 43-fold, with a 10% probability for an increase >43-fold relative to the base period. The increase for 2046–2065 is −1- to 35-fold under RCP8.5-SSP3 and −1- to 31-fold under RCP4.5-SSP2 for the same probability. The changes are much smaller for 2016–2035 than for 2046–2065, with >70% probability of a zero-to 7-fold increase for the three scenarios. The change for 2046–2065 is largest under RCP2.6-SSP1, with nearly a 15% probability of a >15-fold increase relative to the base period, whereas the increases are 7- and 11-fold under the RCP4.5-SSP2 and RCP8.5-SSP3 scenarios, respectively, for the same probability.

4. Discussion

4.1. Impact of a warmer climate on socioeconomic exposure to extreme heat

Our study shows spatiotemporal variation and changes in exposure and its components at global and continental levels. The results indicate variations among the continents (Figs. S4 and S5). For example, population exposure is highest in Asia (Fig. S4), accounting for >50% of the global exposure, followed by Africa, North America, Europe, South America, and Oceania. The percent of population exposure for Africa and South America is projected to increase over time and with an increase in GHG emissions, whereas the percentage of population exposure for Asia, Europe, and North America is projected to decrease over time. GDP exposure accounted for >50% of the total exposure for Asia (Fig. S5), with likely increases under the future scenarios, followed by North America, Europe, Africa, South America, and Oceania. The percent of exposure for developing countries, such as in Africa and South America, increases for the future scenarios. In contrast, decreases would be likely for developed countries, such as those in North America, Europe, and Oceania. Extreme heat under climate change would thus affect Asia the most, where population and GDP exposures are highest. Exposure for Africa is expected to increase rapidly in the future. Therefore, more attention should be directed to Asia and Africa for deeper research on extreme heat exposure and risk assessment. In addition, the design and implementation of effective adaptive measures are urgently needed in regions with high socioeconomic exposure, to lessen populations suffering from heat extremes and reduce the economic losses under climate change.

We estimate future socioeconomic exposure based on SSP projections with to various RCP scenarios. Because the current data are well understood and widely accepted, however, some previous research is based on current spatial distributions and population and GDP exposures (Hsiang et al., 2017). We also calculate exposure to future extreme heat regardless of changes in population and GDP (Table S3). The results indicate that socioeconomic exposure would increase significantly under climate change, with distinct differences among the RCP scenarios, even if population and GDP exposures are maintained at current levels. Exposure is lowest under the RCP2.6 scenario and highest under the RCP8.5 scenario. Population and GDP exposures are 1.72- and 1.67-fold higher under RCP8.5 than under RCP2.6, respectively. Both results for the SSP projections and the current fixed values highlight the importance of reducing emissions. Overall, it is potential to mitigate the impact of climate change on both extreme heat hazards and population exposures under the RCP2.6 scenario compared to RCP4.5 and 8.5 scenarios. And the efficiency of reducing emissions should be further quantified in future studies under RCP2.6 or other ambitious warming target, such as 1.5 °C and 2 °C warming target proposed in Paris Agreement (UNFCCC, 2015), which will be helpful for making climate change mitigation strategies.

4.2. Uncertainty, limitation and further research

Heat extremes could be measured by using different thresholds (e.g., 90, 95, 97.5, and 99th percentile of daily maximum temperatures over the base period). The spatial patterns of exposure and change are generally similar, whereas the quantity of exposure and the relative importance of factors differ greatly (Liu et al., 2017). Assessing socioeconomic exposure under climate change has many uncertainties, except for the indices that measure extreme heat.

The primary sources of uncertainty include scenarios of GHG emission (Maurer, 2007), GCMs (Soden et al., 2018), predictions of population and GDP (Chen et al., 2018) and the calculation method of exposure (Zhang et al., 2018b). The research of Bonan and Doney (2018) on global change in stresses on terrestrial and marine ecosystems show that the uncertainty on land is mostly from model uncertainty, which contributes nearly 80% of the total uncertainty in the 21st century. We evaluate population and GDP exposures based on five GCM simulations after downscaling and assessing the various scenarios and time periods separately. Figs. 4–7 show the differences between the GCMs. In addition to displaying the mean value of five GCMs, the standard deviation of five GCMs is also displayed as error bars in the figures. This study generates assessments by considering different sources of uncertainty, so the results can be considered as reasonable with relatively high accuracy.

This study is also subject to some limitations. First, our study quantified spatiotemporal variation of population and GDP exposures to extreme heat as an important first step for estimating changes in risk, which made progress compared to the previous studies ignoring the spatiotemporal variation of the socioeconomic risk (Barnett et al., 2012; Gasparrini and Armstrong, 2011; Voorhees et al., 2011). However, we do not estimate changes in vulnerability due to the lack of more advanced damage data due to heat extremes. In further studies, we should also concentrate on assessing vulnerability when the data are available, which is also essential for assessing risk. In addition, adopting measures such as the use of air conditioning and the purchase of insurance should be taken into account. These factors would likely improve resilience to heat extremes and thus decrease vulnerability and limit the impact of climate change. Second, the effect of urban heat islands (UHIs) in addition to global warming is not considered explicitly in the climate change simulations in this study. UHIs are confirmed to exacerbate the extent and intensity of heat extremes in urban areas and increase the risk to urban residents in heat extremes (Dan and Bou-Zeid, 2013; Hajat and Kosatky, 2010; Mishra et al., 2015). Recently, as the importance of urbanization in climate change has come to be realized, several case studies simulating the impact of urbanization on extreme temperature events been done (Chen and Frauenfeld, 2016; Grossman-Clarke et al., 2010; Wang et al., 2012). Some research focused on intensely urbanized places such as eastern China, the eastern USA, and Western Europe, which is consistent with the results of our studies on high-exposure regions. However, some other regions such as western Africa and northern India are also expected to suffer high exposure to heat extremes in the future. More attention should be focused on these regions in future studies (see Fig. 8). However, global studies are rare because of a lack of precise land-use and population data. Some other studies assess the future urban climate change by using GCM (Fischer et al., 2012; Oleson, 2012). However, given the coarse spatial resolution, the influence of GCM on underlying urban surfaces could not be fully appreciated, so the impact of future urban development on UHIs was not considered in these studies. As a result, the effect of UHIs on extreme temperature events may be underestimated. Therefore, in future studies, the design and nesting of urban land surface models and the estimation of UHI, especially the heat island estimation during heat extremes, should be taken into account, since they are critical for estimating exposure and risk to heat extremes in cities due to climate change.

5. Conclusions

This study generated four key findings. First, the regions with the highest population and GDP exposures to extreme heat are primarily concentrated in densely populated areas, such as India, China, midwestern Europe, the eastern USA, and the coastal areas of South America. Second, global population exposure for the years 2046–2065 is highest under the RCP8.5-SSP3 scenario, with exposure increasing 3.76-fold relative to the base period 1986–2005. The RCP2.6-SSP1 scenario produces the highest global GDP exposure, with exposure increasing 10.47-fold for 2046–2065. Third, exposure is highest for Asia for both population and GDP, which exceeds 50% of the global exposure. The increase in exposure

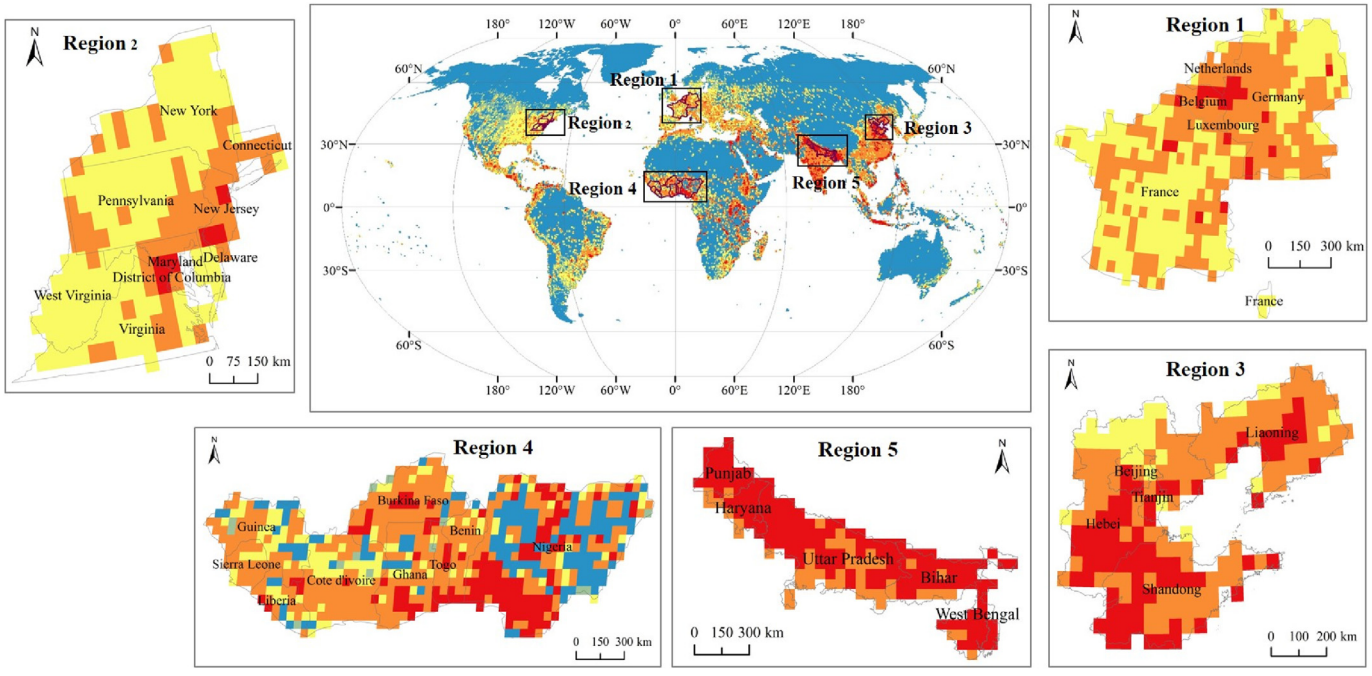

Fig. 8. Regions with high future exposure under climate change. E.g. Western Europe (region 1), the eastern USA (region 2), eastern China (region 3), western Africa (region 4) and northern India (region 5), may face more risk in heat extremes coupled with the effect of urban heat islands in intensely urbanized places.

is largest for Africa, with the annual population and GDP exposures 9.20- and 29.34-fold higher, respectively, than during the base period. In contrast, the relative changes in population and GDP exposures are lowest for Europe and North America, respectively. Fourth, the effect of climate is the dominant contribution globally to change in population exposure, accounting for nearly half of the total change (47%–53%). The effect of GDP is responsible for nearly 50% of the total change in GDP exposure for 2016–2035, whereas the interactive effect makes the primary contribution for 2046–2065 under the RCP4.5-SSP2 and RCP8.5-SSP3 scenarios, accounting for 49% and 53% of the total change, respectively. In conclusion, mitigating emissions of greenhouse gases, either at the level of the RCP2.6 scenario or at a more ambitious target of reduction, is important for reducing socioeconomic exposure to heat extremes. In addition, designing and implementing effective measures of adaptation are urgently needed in Asia and Africa to aid socioeconomic systems suffering from heat extremes due to climate change.

CRediT authorship contribution statement

Jie Chen: Formal analysis, Methodology, Writing - original draft. **Yujie Liu:** Conceptualization, Investigation, Funding acquisition, Project administration, Resources, Supervision, Writing - review & editing. **Tao Pan:** Supervision, Writing - review & editing. **Philippe Ciais:** Writing - review & editing. **Ting Ma:** Data curation, Writing - review & editing. **Yanhua Liu:** Supervision. **Dai Yamazaki:** Writing - review & editing. **Quansheng Ge:** Supervision. **Josep Peñuelas:** Writing - review & editing.

Declaration of competing interest

The authors declare that they have no conflict of interest.

Acknowledgments

This study was supported by the National Key Research and Development Program of China (Grant No. 2016YFA0602402); the Youth Innovation Promotion Association, CAS (Grant No. 2016049); the Program for “Kezhen” Excellent Talents in Institute of Geographic Sciences and Natural Resources Research (IGSNRR), CAS, (Grant No. 2017RC101); the Key Research Program of Frontier Sciences, CAS (Grant No. QYZDB-SSW-DQC005); and the ERC-SyG-2013-610028 IMBALANCE-P. We also thank ISI-MIP and NIES for data support.

Appendix A. Supplementary data

Supplementary data to this article can be found online at https://doi.org/10.1016/j.jclepro.2020.123275.

References

Barnett, A.G., Tong, S., Clements, A.C.A., 2012. What measure of temperature is the best predictor of mortality? Environ. Res. 118, 149–151. https://doi.org/10.1016/j.envres.2010.05.006.

Bonan, G.B., Doney, S.C., 2018. Climate, ecosystems, and planetary futures: the challenge to predict life in Earth system models. Science 359 (6375), eaam8328. https://doi.org/10.1126/science.aam8328.

Bouwer, L.M., 2013. Projections of future extreme weather losses under changes in climate and exposure. Risk Anal. 33, 915–930. https://doi.org/10.1111/j.1539-6924.2012.01880.x.

Bowles, D.C., Butler, C.D., Friel, S., 2014. Climate change and health in Earth’s future. Earths Future 2, 60–67. https://doi.org/10.1002/2013EF000177.

Burke, M., Hsiang, S.M., Miguel, E., 2015. Global non-linear effect of temperature on economic production. Nature 527, 235–239. https://doi.org/10.1038/nature15725.

Carleton, T.A., Hsiang, S.M., 2016. Social and economic impacts of climate. Science 353. https://doi.org/10.1002/2014GL061859 aad9837–aad9837. 10.1126/science.aad9837.

Ceola, S., Laio, F., Montanari, A., 2015. Satellite nighttime lights reveal increasing human exposure to floods worldwide. Geophys. Res. Lett. 41, 7184–7190. https://doi.org/10.1002/2014GL061859.

Chen, J., Liu, Y., Pan, T., Liu, Y., Sun, F., Ge, Q., 2018. Population exposure to droughts in China under the 1.5° C global warming target. Earth Syst Dynam 9 (3), 1097–1106. https://doi.org/10.5194/esd-9-1097-2018.

Chen, L., Frauenfeld, O.W., 2016. Impacts of urbanization on future climate in China. Clim. Dynam. 47, 345–357. https://doi.org/10.1007/s00382-015-2840-6.

Cook, B.I., Smerdon, J.E., Seager, R., Coats, S., 2014. Global warming and 21st century drying. Clim. Dynam. 43, 2607–2627. https://doi.org/10.1007/s00382-014-2075-y.

Dan, L., Bou-Zeid, E., 2013. Synergistic interactions between urban heat islands and heat waves: the impact in cities is larger than the sum of its parts. J Appl Meteorol Clim 52, 2051–2064. https://doi.org/10.1175/JAMC-D-13-02.1.

Field, C.B., Barros, V., Stocker, T.F., 2012. Managing the risks of extreme events and disasters to advance climate change adaptation. In: Special Report of the Intergovernmental Panel on Climate Change (IPCC). Cambridge University Press.

Fischer, E.M., Knutti, R., 2015. Anthropogenic contribution to global occurrence of heavy-precipitation and high-temperature extremes. Nat. Clim. Change 5, 560–564. https://doi.org/10.1038/nclimate2617.

Fischer, E.M., Oleson, K.W., Lawrence, D.M., 2012. Contrasting urban and rural heat stress responses to climate change. Geophys. Res. Lett. 39, L03705. https://doi.org/10.1029/2011GL050576.

Forzieri, G., Cescatti, A., Silva, F.B.E., Feyen, L., 2017. Increasing risk over time of weather-related hazards to the European population: a data-driven prognostic study. Lancet Planet Health 1. https://doi.org/10.1016/S2542-5196(17)30082-7 e200–e208.

Garssen, J., Harmsen, C., De, B.J., 2005. The effect of the summer 2003 heat wave on mortality in The Netherlands. Euro Surveill. 10, 165–168. https://doi.org/10.2807/esm.10.07.00557-en.

Gasparrini, A., Armstrong, B., 2011. The impact of heat waves on mortality. Epidemiology 22, 68–73. https://doi.org/10.1097/ede.0b013e3181fdcd99.

Gasparrini, A., et al., 2015. Mortality risk attributable to high and low ambient temperature: a multicountry observational study. Lancet 386, 369–375. https://doi.org/10.1016/S0140-6736(14)62114-0.

Grossman-Clarke, S., Zehnder, J.A., Loridan, T., Grimmond, C.S.B., 2010. Contribution of land use changes to near-surface air temperatures during recent summer extreme heat events in the Phoenix metropolitan area. J Appl Meteoro Clim 49, 1649–1664. https://doi.org/10.1175/2010jamc2362.1.

Hajat, S., Kosatky, T., 2010. Heat-related mortality: a review and exploration of heterogeneity. J. Epidemiol. Community Health 64, 753–760. https://doi.org/10.1136/jech.2009.087999.

Harrington, L.J., Otto, F.E.L., 2018. Changing population dynamics and uneven temperature emergence combine to exacerbate regional exposure to heat extremes under 1.5 °C and 2 °C of warming. Environ. Res. Lett. 13, 034011 https://doi.org/10.1088/1748-9326/aaaa99.

Hempel, S., Frieler, K., Warszawski, L., Schewe, J., Piontek, F., 2013. A trend-preserving bias correction - the ISI-MIP approach. Earth Syst Dynam 4, 219–236. https://doi.org/10.5194/esd-4-219-2013.

Hirabayashi, Y., et al., 2013. Global flood risk under climate change. Nat. Clim. Change 3, 816–821. https://doi.org/10.1038/nclimate1911.

Hsiang, S., et al., 2017. Estimating economic damage from climate change in the United States. Science 356, 1362–1369. https://doi.org/10.1126/science.aal4369.

Huang, J., et al., 2017. Analysis of future drought characteristics in China using the regional climate model CCLM. Clim. Dynam. 50, 507–525. https://doi.org/10.1007/s00382-017-3623-z.

IPCC, 2013. Climate Change 2013: the Physical Science Basis. Contribution of Working Group I to the Fifth Assessment Report of the Intergovernmental Panel on Climate Change. Cambridge University Press, Cambridge, UK, New York, USA.

IPCC, 2014. Climate Change 2014: Impacts, Adaptation, and Vulnerability. Part A: Global and 248 Sectoral Aspects. Contribution of Working Group II to the Fifth Assessment Report of the 249 Intergovernmental Panel on Climate Change. Cambridge University Press, Cambridge, UK, New York, USA.

Jones, B., O’Neill, B.C., 2016. Spatially explicit global population scenarios consistent with the Shared Socioeconomic Pathways. Environ. Res. Lett. 11, 084003 https://doi.org/10.1088/1748-9326/11/8/084003, 2016.

Jones, B., O’Neill, B.C., Mcdaniel, L., Mcginnis, S., Mearns, L.O., Tebaldi, C., 2015. Future population exposure to US heat extremes. Nat. Clim. Change 5, 592–597. https://doi.org/10.1038/nclimate2631.

Kharin, V.V., Zwiers, F.W., Zhang, X., Wehner, M., 2013. Changes in temperature and precipitation extremes in the CMIP5 ensemble. Climatic Change 119, 345–357. https://doi.org/10.1007/s10584-013-0705-8.

King, A.D., Karoly, D.J., Henley, B.J., 2017. Australian climate extremes at 1.5° C and 2° C of global warming. Nat. Clim. Change 7, 412–416. https://doi.org/10.1038/nclimate3296.

Liu, Z., Anderson, B., Yan, K., Dong, W., Liao, H., Shi, P., 2017. Global and regional changes in exposure to extreme heat and the relative contributions of climate and population change. Sci. Rep. 7, 43909. https://doi.org/10.1038/srep43909.

Maurer, E.P., 2007. Uncertainty in hydrologic impacts of climate change in the Sierra Nevada, California, under two emissions scenarios. Climatic Change 82, 309–325. https://doi.org/10.1007/s10584-006-9180-9.

Mishra, V., Ganguly, A.R., Nijssen, B., Lettenmaier, D.P., 2015. Changes in observed

climate extremes in global urban areas. Environ. Res. Lett. 10, 024005 https://doi.org/10.1088/1748-9326/10/2/024005.
Mishra, V., Mukherjee, S., Kumar, R., Stone, D.A., 2017. Heat wave exposure in India in current, 1.5 °C, and 2.0 °C worlds. Environ. Res. Lett. 12, 124012. https://doi.org/10.1088/1748-9326/aa9388.
Mora, C., et al., 2017. Global risk of deadly heat. Nat. Clim. Change 7, 501–506. https://doi.org/10.1038/nclimate3322.
Murakami, D., Yamagata, Y., 2016. Estimation of gridded population and GDP scenarios with spatially explicit statistical downscaling. available at: https://arxiv.org/abs/1610.09041.
Nath, R., et al., 2017. CMIP5 multimodel projections of extreme weather events in the humid subtropical Gangetic Plain region of India. Earths Future 5, 224–239. https://doi.org/10.1002/2016EF000482.
O'Neill, B.C., et al., 2014. A new scenario framework for climate change research: the concept of shared socioeconomic pathways. Climatic Change 122, 401–414. https://doi.org/10.1007/s10584-013-0905-2.
Oleson, K., 2012. Contrasts between urban and rural climate in CCSM4 CMIP5 climate change scenarios. J. Clim. 25, 1390–1412. https://doi.org/10.1175/JCLI-D-11-00098.1.
Riahi, K., et al., 2017. The shared socioeconomic pathways and their energy, land use, and greenhouse gas emissions implications: an overview. Global Environ. Change 42, 153–168. https://doi.org/10.1016/j.gloenvcha.2016.05.009.
Robine, J.M., Cheung, S.L.K., Roy, S.L., Oyen, H.V., Griffiths, C., Michel, J.P., Herrmann, F.R., 2008. Death toll exceeded 70,000 in Europe during the summer of 2003. C. R. Biol. 331, 171–178. https://doi.org/10.1016/j.crvi.2007.12.001.
Schleussner, C.F., Lissner, T.K., Fischer, E.M., Wohland, J., Perrette, M., Golly, A., Rogelj, J., Childers, K., Schewe, J., Frieler, K., 2016. Differential climate impacts for policy-relevant limits to global warming: the case of 1.5 °C and 2 °C. Earth Syst Dynam 6, 2447–2505. https://doi.org/10.5194/esd-7-327-2016.
Smirnov, O., Zhang, M., Xiao, T., Orbell, J., Lobben, A., Gordon, J., 2016. The relative importance of climate change and population growth for exposure to future extreme droughts. Climatic Change 138, 1–13. https://doi.org/10.1007/s10584-016-1716-z.
Soden, B.J., Collins, W.D., Feldman, D.R., 2018. Reducing uncertainties in climate models. Science 361, 326–327. https://doi.org/10.1126/science.aau1864.
Sun, H., et al., 2017. Exposure of population to droughts in the Haihe River Basin under global warming of 1.5 and 2.0°C scenarios. Quat. Int. 53, 74–84. https://doi.org/10.1016/j.quaint.2017.05.005.
Sun, Y., et al., 2014. Rapid increase in the risk of extreme summer heat in Eastern China. Nat. Clim. Change 4, 1082–1085. https://doi.org/10.1038/nclimate2410.
Taylor, K.E., Stouffer, R.J., Meehl, G.A., 2012. An overview of CMIP5 and the experiment design. Bull. Am. Meteorol. Soc. 93, 485–498. https://doi.org/10.1175/BAMS-D-11-00094.1.
Trenberth, K.E., Fasullo, J.T., 2012. Climate extremes and climate change: the Russian heat wave and other climate extremes of 2010. J. Geophys. Res. Atmos. 117, D17103. https://doi.org/10.1029/2012JD018020.
UNFCCC Conference of the Parties (COP), 2015. Adoption of the Paris Agreement (Paris, France).
Vaneckova, P., Beggs, P.J., de Dear, R.J., Mccracken, K.W., 2008. Effect of temperature on mortality during the six warmer months in Sydney, Australia, between 1993 and 2004. Environ. Res. 108, 361–369. https://doi.org/10.1016/j.envres.2008.07.015.
Voorhees, A.S., Fann, N., Fulcher, C., Dolwick, P., Hubbell, B., Bierwagen, B., Morefield, P., 2011. Climate change-related temperature impacts on warm season heat mortality: a proof-of-concept methodology using BenMAP. Environ. Sci. Technol. 45, 1450–1457. https://doi.org/10.1021/es102820y.
Vuuren, D.P.V., et al., 2011. The representative concentration pathways: an overview. Climatic Change 109, 5–31. https://doi.org/10.1007/s10584-011-0148-z.
Wang, J., Feng, J., Yan, Z., Hu, Y., Jia, G., 2012. Nested high-resolution modeling of the impact of urbanization on regional climate in three vast urban agglomerations in China. J. Geophys. Res. Atmos. 117, D21103. https://doi.org/10.1029/2012JD018226.
Wang, Y., Wang, A., Zhai, J., Tao, H., Jiang, T., Su, B., Fischer, T., 2019. Tens of thousands additional deaths annually in cities of China between 1.5 °C and 2.0 °C warming. Nat. Commun. 10 (1), 3376. https://doi.org/10.1038/s41467-019-11283-w.
Warszawski, L., Frieler, K., Huber, V., Piontek, F., Serdeczny, O., Schewe, J., 2014. The inter-sectoral impact model intercomparison project (ISI-MIP): project framework. Proc. Natl. Acad. Sci. U.S.A. 111, 3228–3232. https://doi.org/10.1073/pnas.1312330110.
Zhang, W., Zhou, T., Zou, L., Zhang, L., Chen, X., 2018b. Reduced exposure to extreme precipitation from 0.5 °C less warming in global land monsoon regions. Nat. Commun. 9 (1), 3153. https://doi.org/10.1038/s41467-018-05633-3.
Zhang, Z., Li, N., Xu, H., Chen, X., 2018a. Analysis of the economic ripple effect of the United States on the world due to future climate change. Earths Future 6, 828–840. https://doi.org/10.1029/2018EF000839.